Supplementary Information for

First-Principles Exploration of Oxygen Vacancy Impact on Electronic and Optical Properties of $ABO_{3-\delta}$ (A = La, Sr; B = Cr, Mn) Perovskites

Jongwoo Park[1], Yu-Ning Wu[1], Wissam A. Saidi[1,2], Benjamin Chorpening[1], and Yuhua Duan[1*]

[1] National Energy Technology Laboratory, United States Department of Energy, Pittsburgh, PA 15236 USA

[2] Department of Mechanical Engineering and Materials Science, University of Pittsburgh, Pittsburgh, PA 15261 USA

[*] Corresponding author. E-mail: yuhua.duan@netl.doe.gov.

Table of Contents

S1. Oxygen Vacancy Formation Energy

Tables S1 - S4 curate the numerical data of the formation energy of oxygen mono-vacancy in ABO_3 (A = La, Sr, B = Cr, Mn) perovskites with different valence charges as a function of Fermi level shwon in Fig. 2 of the main text.

Table S1. Formation energy of oxygen mono-vacancy (ΔH^q) employing different vacancy charge states (q) as a function of Fermi level (E_F) for $LaCrO_3$ (Fig. 2a).

$q = 0$ (v_O^0) *		$q = 1+$ (v_O^{1+})		$q = 2+$ (v_O^{2+})	
E_F (eV)	ΔH^q (eV)	E_F (eV)	ΔH^q (eV)	E_F (eV)	ΔH^q (eV)
0.00	4.95	0.00	4.05	0.00	3.15
0.25	4.95	0.25	4.30	0.25	3.65
0.50	4.95	0.50	4.55	0.50	4.15
0.75	4.95	0.75	4.80	0.75	4.65
1.00	4.95	1.00	5.05	1.00	5.15
1.25	4.95	1.25	5.30	1.25	5.65
1.50	4.95	1.50	5.55	1.50	6.15

* Due to the nature of eqn. (1) discussed in the main text, ΔH^q does not vary with E_F when $q = 0$.

Table S2. Formation energy of oxygen mono-vacancy (ΔH^q) employing different vacancy charge states (q) as a function of Fermi level (E_F) for $LaMnO_3$ (Fig. 2b).

$q = 0$ (v_O^0) *		$q = 1+$ (v_O^{1+})		$q = 2+$ (v_O^{2+})	
E_F (eV)	ΔH^q (eV)	E_F (eV)	ΔH^q (eV)	E_F (eV)	ΔH^q (eV)
0.00	3.48	0.00	3.32	0.00	3.30
0.10	3.48	0.10	3.42	0.10	3.50
0.20	3.48	0.20	3.52	0.20	3.70
0.30	3.48	0.30	3.62	0.30	3.90
0.40	3.48	0.40	3.72	0.40	4.10
0.50	3.48	0.50	3.82	0.50	4.30

* Due to the nature of eqn. (1) discussed in the main text, ΔH^q does not vary with E_F when $q = 0$.

Table S3. Formation energy of oxygen mono-vacancy (ΔH^q) employing different vacancy charge states (q) as a function of Fermi level (E_F) for $SrCrO_3$ (Fig. 2c).

$q = 0$ (v_O^0) *		$q = 1+$ (v_O^{1+})		$q = 2+$ (v_O^{2+})	
E_F (eV)	ΔH^q (eV)	E_F (eV)	ΔH^q (eV)	E_F (eV)	ΔH^q (eV)
0.00	4.32	0.00	3.93	0.00	3.53
0.25	4.32	0.25	4.18	0.25	4.03
0.50	4.32	0.50	4.43	0.50	4.53
0.75	4.32	0.75	4.68	0.75	5.03
1.00	4.32	1.00	4.93	1.00	5.53

* Due to the nature of eqn. (1) discussed in the main text, ΔH^q does not vary with E_F when $q = 0$.

Table S4. Formation energy of oxygen mono-vacancy (ΔH^q) employing different vacancy charge states (q) as a function of Fermi level (E_F) for $SrMnO_3$ (Fig. 2d).

$q = 0$ (v_O^0) *		$q = 1+$ (v_O^{1+})		$q = 2+$ (v_O^{2+})	
E_F (eV)	ΔH^q (eV)	E_F (eV)	ΔH^q (eV)	E_F (eV)	ΔH^q (eV)
0.00	1.48	0.00	1.05	0.00	0.78
0.20	1.48	0.20	1.25	0.20	1.18
0.40	1.48	0.40	1.45	0.40	1.58
0.60	1.48	0.60	1.65	0.60	1.98
0.80	1.48	0.80	1.85	0.80	2.38
1.00	1.48	1.00	2.05	1.00	2.78

* Due to the nature of eqn. (1) discussed in the main text, ΔH^q does not vary with E_F when $q = 0$.

S2. Electronic Band Structures of Oxygen-Vacant $LaCrO_3$ and $LaMnO_3$

Fig. S1 shows the electronic band structures, and atom- and angular-momentum projected PDOS for oxygen-vacant $LaCrO_3$ and $LaMnO_3$ with different vacancy charges discussed in Fig. 4 of the main text. PDOS of oxygen-vacant v_O^q states of $LaCrO_3$ and $LaMnO_3$ are reproduced from Fig. 4 for complete comparisons.

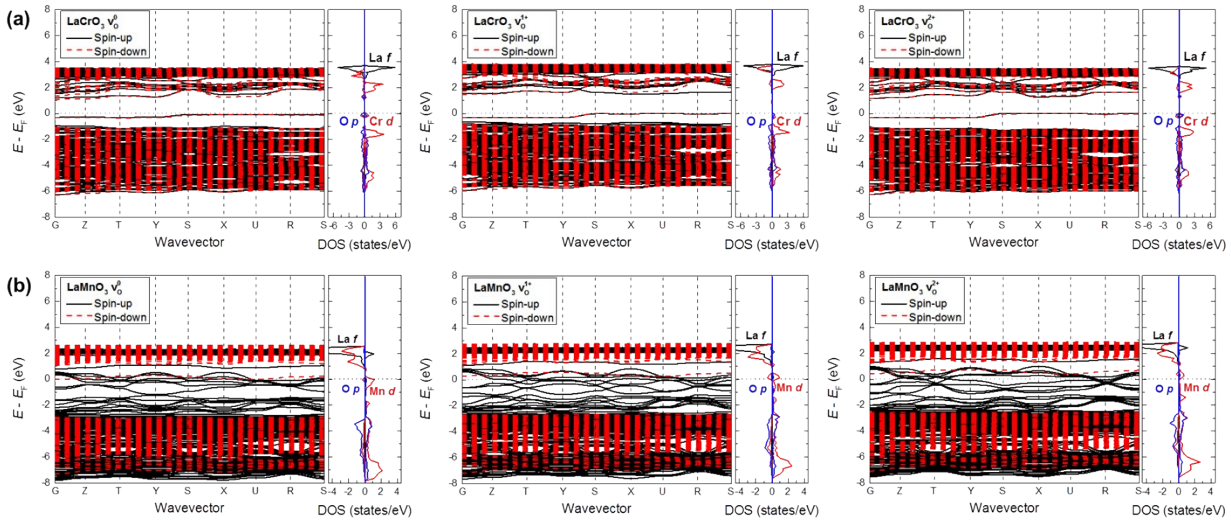

Fig. S1. Electronic band structures along the high-symmetry paths in the first Brillouin zones and PDOS for oxygen-vacant (a) $LaCrO_3$ v_O^q and (b) $LaMnO_3$ v_O^q. Zero of the energy (E) scale is position of the Fermi level (E_F) set in the middle between the band edges.

Fig. S2 shows the electronic charge density displaying the density of electrons in pristine and oxygen-vacant $LaCrO_3$ and $LaMnO_3$ to examine the electron distribution of these systems.[1] The charge density isovalue is higher in pristine $LaCrO_3$ than in $LaMnO_3$. In each material, the charge density isovalues are increased (i.e. when closing to the nuclues of atoms) in oxygen-vacant systems relative to the corresponding pristine materials. Nonetheless the impact of neutral and/or charged vacancy on their charge density maps is not eyecatching.

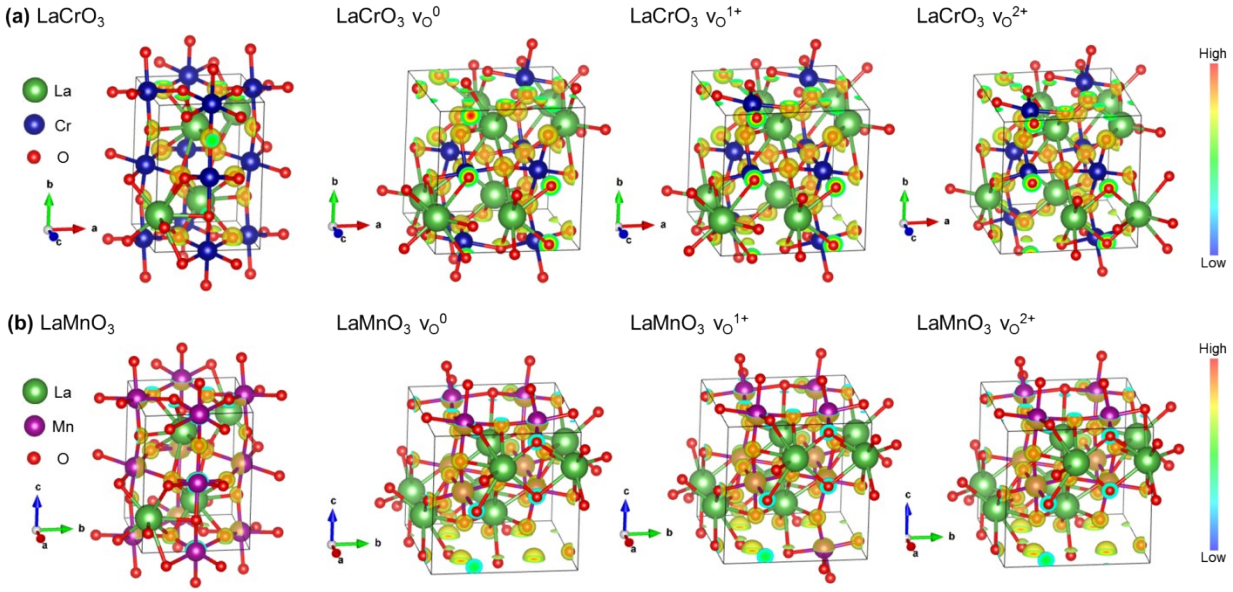

Fig. S2. Charge density maps for (a) AFM-G magnetic ordered $LaCrO_3$ (v_O^q) and (b) FM magnetic ordered $LaMnO_3$ (v_O^q). The maps are shown with primitive cells for pristine $LaCrO_3$ and $LaMnO_3$, and with 2 × 1 × 1 supercells for oxygen-vacant $LaCrO_3$ v_O^q and $LaMnO_3$ v_O^q. Charge density in space is depicted by smooth shadings with the color scheme (indicated with a bar on the right) for the charge density isovalue.

References

1 C. Gatti and P. Macchi, *A Guided Tour Through Modern Charge Density Analysis. In Modern Charge-Density Analysis*, Springer, Dordrecht, 2011.